1973

Evaluation of st. Venant torsional constants for prestressed concrete i-beams, September 1973

Clifford C. Eby

John M. Kulicki

C. N. Kostem

Martin A. Zellin

THE EVALUATION OF ST. VENANT TORSIONAL CONSTANTS

FOR PRESTRESSED CONCRETE I-BEAMS

by

Clifford C. Eby

John M. Kulicki

Celal N. Kostem

Martin A. Zellin

Fritz Engineering Laboratory

Department of Civil Engineering

Lehigh University

September 1973

Fritz Engineering Laboratory Report No. 400.12

ERRATA:

1. Page 13, Equation (21) is missing.

2. Page 13, Equations (22), (23) and (19) should be Equations (21), (22) and (23), respectively.

3. Page 14, equation (24-B) is missing the factor of 2 in the denominator.

TABLE OF CONTENTS

ABSTRACT

This report contains the results of a study to determine the St. Venant torsional constant for twenty-five I-shaped cross-sections commonly used as prestressed concrete bridge beams. Results obtained by a finite difference analysis are compared to torsional constants computed using six approximate methods. One of these methods is shown to provide an excellent approximation for the shapes investigated.

Results are also presented for seven other cross-sections used as test examples for the finite difference computer program. The calculated torsional constants agree very well with the accepted solutions.

Torsional shear stress coefficients are tabulated for three points on each of the twenty-five beam cross-sections.

1. INTRODUCTION

1.1 Objective

This report contains the results of a pilot study undertaken to evaluate the St. Venant torsional constant, K_T, and shear stress coefficients for cross-sections used as prestressed concrete I-beams. AASHO Types I, through VI cross-sections and the nineteen standard sections currently or previously used by the Pennsylvania Department of Transportation were investigated (Refs. 2,3,9). Only the basic concrete section was considered. Figure 1 shows a typical I-shape and Table 1 contains the dimensions of the sections which were investigated. The dimensions for the AASHO Types V and VI beams are idealized to fit the basic I-shape shown in Fig. 1. Reference 2 contains the true dimensions. The results presented for these two sections should be considered as somewhat more approximate than those for the other sections.

Seven different methods were used to compute the torsional constants. The primary method under consideration is a numerical solution of the governing differential equation using finite differences. The resulting equations were solved to find values of the torsional stress function at discrete mesh points, referred to as points in the report. The torsional constant was then evaluated by integrating the stress function over the cross-section by trapazoidal rule with special consideration of edge points. Details of the analytic procedure are presented in Chapter 2. The remaining six methods of computing K_T involve the application of well known equations used for simpler shapes.

These equations are used as a check on the finite difference results. It is also determined if any of these six methods yields results which are consistently closer to the finite difference results than the other methods.

The torsional constants presented herein were developed for use with an existing finite element program for the analysis of eccentrically stiffened plates as described in Refs. 4 and 12. This program is currently being used as the basis for research into the lateral distribution of live load in bridges composed of reinforced concrete decks supported by prestressed concrete I-beams. The St. Venant torsional constant of the I-beam cross-section is used as input to this program and appears in the stiffness matrix of the eccentric beam elements. A literature survey has shown the need to include K_T in a lateral load distribution analysis technique (Ref. 13).

1.2 Previous Work

1.2.1 The Membrane Analogy

The membrane analogy proposed by Prandtl for solving for the torsional constant and shear stresses is used here. This analogy is based on the similarities existing between the differential equations defining the St. Venant torsion problem and the shape of a thin inflated membrane stretched over a hole shaped like the cross-section under investigation. The result is that, as stated in Ref. 6:

"1. The stress function ϕ, which is a measure of the torsional deformation is analogous to the deflection ... of the membrane.

2. The shear stresses due to torsion correspond to the slopes of the membrane, and

3. The volume under the membrane is related to the twisting moment."

The result is that the following set of equations can be used to define the torsion problem (Ref. 11)

a matter of how ϕ is defined

$$\frac{\partial^2 \phi}{\partial x^2} + \frac{\partial^2 \phi}{\partial y^2} = -2 \quad \text{In the Region} \qquad (1)$$

$$\phi = 0.0 \quad \text{On the Boundary} \qquad (2)$$

$$K_T = 2 \int_x \int_y \phi \, dx \, dy \qquad (3)$$

$$\tau_{xz} = \frac{T}{K_T} \frac{\partial \phi}{\partial y} , \quad \tau_{yz} = - \frac{T}{K_T} \frac{\partial \phi}{\partial x}$$

T is the applied torque, τ_{xz} and τ_{yz} are shear stresses, x and y are reference axes in the plane of the cross-section and z is the coordinate perpendicular to the cross-section.

1.2.2 Presentation of Approximate Equations

St. Venant's solution for a rectangular shape can be written as (Ref. 8)

$$K_T = \frac{bt^3}{3} - 2\ Vt^4 \tag{4}$$

In Eq. 4, b is the larger dimension and t the smaller dimension of the cross-section. Tables of V, an end slope reduction factor, are available in Refs. 5 and 7. Equation 4 is sometimes approximated as Eq. 5 (Ref. 1).

$$K_T \simeq \frac{bt^3}{3} \left[1.0 - 0.63\ \frac{t}{b} + 0.052\ \left(\frac{t}{b}\right)^2\right] \tag{5}$$

As the rectangular section becomes thinner Eqs. 4 and 5 approach Eq. 6 which is also sometimes used as an approximation.

$$K_T \simeq \frac{bt^3}{3} \tag{6}$$

St. Venant also developed an approximation for the torsional constant which can be applied to a wide variety of solid sections (Ref. 7). This approximation is given by Eq. 7

$$K_T \simeq \frac{A^4}{40\ Ip} \tag{7}$$

Ip is the polar moment of inertia of the section and A is its area. Reference 7 also contains a comparison of exact torsional constants and the approximate values given by Eq. 7 for a variety of solid sections. Reentrant corners are not permitted in the application of St. Venant's approximate formula unless the area is subdivided into smaller areas which do not contain reentrant corners. This is discussed in Chapter 3.

Lyse and Johnston (Ref. 8) developed an equation for trapazoidal sections corresponding to Eq. 4. This is given as Eq. 8.

$$K_T = \left(\frac{b}{12}\right) (t_1^2 + t_2^2)(t_1 + t_2) - V_L t_2^4 - V_S - V_S t_1^4 \tag{8}$$

t_1 is the smaller parallel dimension of the trapazoid and t_2 is the larger. V_L is the end slope correction for the wider and V_S is the end slope correction for the smaller end.

Equations 4, 5, 6, 7 and 8 could be used to develop torsional constants for open sections composed of rectangles and trapazoids by adding up the various contributions to the constant. Applications of Eqs. 5, 6 and 7 form four of the six approximate methods used here. There are also stiffening effects associated with the junction of the rectangles and/or trapazoids and with fillets if any are present. Trayer and March (Ref. 10) suggested that these additional contributions to torsional stiffness be taken as some factor times the fourth power of the diameter of the largest circle which can be inscribed in the junction. Reference 8 contains values for this factor for some structural shapes. These values were determined by measuring the volume under experimental membranes and comparing the results with the torsional constant found by summing up the individual contributions. Reference 5 contains more recent work based on finite differences in which a calculated torsional constant was compared with the sum of individual contributions. Equations for many structural shapes are presented which give the torsional constant in terms of the individual contributions, end slope corrections and junction and fillet corrections. El-Darwish and Johnston (Ref. 5) have presented the following equations for the doubly symmetric I-Section shown in Fig. 2.

$$K_T = \frac{2}{3} bt^3 + \frac{1}{3} (d - 2t) w^3 + 2.0 \alpha_1 D_1^4 - 0.420 t^4 \tag{9}$$

$$D_1 = \frac{(t + r)^2 + w \left(r + \frac{w}{4}\right)}{2r + t} \tag{10}$$

t, d, w and r are illustrated in Fig. 2. Reference 5 contains figures relating values of α_1 to w/t for various values of r/t for the case of parallel flanges and for a flange slope of 1:6. For the case of parallel flanges α_1 may be approximated over the interval $0.5 \leq w/t \geq 1.0$ by Eq. 11

$$\alpha_1 = -0.042 + 0.2204 \frac{w}{t} + 0.1355 \frac{r}{t} - 0.0865 \frac{wr}{t^2} - 0.0725 \left(\frac{w}{t}\right)^2 \tag{11}$$

The term $0.420 t^4$ in Eq. 9 is the total end slope correction for both flanges. The value 0.420 is accurate for $b/t > 2.0$ but is adequate for $b/t > 1.4$.

Unfortunately the I-shapes commonly used for prestressed concrete beams are symmetric about only one axis. Furthermore an attempt to provide junction correction factors similar to those found in Refs. 5 and 8 is complicated by additional considerations involving two different flange thicknesses and flange slopes for any given I-beam. Nonetheless a modified version of the results obtained by El-Darwish and Johnston will be applied to twenty-three of the twenty-five sections analyzed by finite differences in this report.

The final approximate method is to consider that $K_T = I_p$. This is true for circles but becomes increasingly less accurate as the given shape deviates from a circle.

1.2.3 Previous Solutions for Prestressed Concrete Beams

Tamberg (Ref. 9) has presented torsional constants and shear stress coefficients for AASHO girders Types I, II, III and IV evaluated by a finite difference approach. Solutions were also presented for beam-slab combinations. Tamberg used far fewer points in the finite difference mesh than was used in this research. The integration scheme consisted of finding areas of sections parallel to the major bending axis by a combination of Simpson's rule and triangular edge pieces. The volume under the membrane was then computed using the average end area method. The results were then increased 5% to compensate for the effect of the large mesh interval on values of ϕ and another 3½% to compensate for the effect of the large mesh interval on the volume calculation. These percentages were chosen based on more exact calculations using the AASHO Type III girder. The results obtained from this previous study are presented in Table II.

2. PRESENTATION OF ANALYSIS TECHNIQUES

2.1 The Finite Difference Analysis

2.1.1 Finite Difference Equations

Each beam to be considered is symmetric about its minor bending axis. Therefore only one-half of each section was analyzed. The process used here closely parallels the finite difference approaches used in Refs. 5 and 9. The region was divided into subareas by a rectangular mesh as shown in Fig. 3-A. Equation 1 can be written in central difference notation for each point using equations from the literature. The particular equations found in Ref. 11 were used here. For a typical interior point such as point 1 in Fig. 3-A the equation for the stress function at that point can be written in terms of the neighboring points defined in Fig. 3-A as:

$$h^2k^2\ \nabla^2\phi_i = k^2\ (\phi_r - 2\phi_i + \phi_\ell) + h^2\ (\phi_a - 2\phi_i + \phi_b) = -2h^2k^2 \tag{12}$$

The variables h and k are defined in Fig. 3-B. For points along the line of symmetry such as point 3:

$$h^2k^2\ \nabla^2\phi_i = k^2\ (2\phi_\ell - \phi_i) + h^2\ (\phi_a - 2\phi_i + \phi_b) = -2h^2k^2 \tag{13}$$

For points along the free edge such as point 2:

$$\phi_i = 0.0 \tag{14}$$

Therefore points along the free edge need not be included in the analysis and will not be included in the count of points used in a given mesh. Only points for which $\phi_i \neq 0.0$ will be included in the count of points.

For points where adjacent points would lie outside the cross-section, such as point 4 in Fig. 3-A, the following equation can be used as appropriate for a given node point.

$$\nabla^2\phi_i = \frac{2}{h\,(h_1 + h)}\,\phi_\ell - 2\left[\frac{1}{kk_1} + \frac{1}{hh_1}\right]\phi_i + \frac{2}{k\,(k + k_1)}\,\phi_b + \frac{2}{k_1\,(k + k_1)}\,\phi_a + \frac{2}{h_1\,(h + h_1)}\,\phi_r = -2 \tag{15}$$

h_1 is the horizontal distance to the face of the cross-section if that distance is less than a whole mesh interval. Likewise k_1 is the vertical distance to the face if that distance is less than a whole mesh interval.

Once the finite difference operators have been written for each point a set of linear algebraic simultaneous equations results. These equations were solved for the value of the stress function at each node point using subroutines available at the Lehigh University Computing Center. A Gauss elimination scheme was employed.

2.1.2 Numerical Integration Technique

The volume under the surface defined by the discrete values of the stress function was found by numerical integration. The point numbers used in Section 2.1.1 and shown in Fig. 3-A will be used in this discussion.

For a point 1, the typical interior point, the contribution to the volume under the stress function could be approximated as:

$$\Delta V \simeq \phi_1 \ (h \cdot k) \tag{16}$$

The product h • k is the area formed by the four quarter mesh areas surrounding a point 1.

For a point 3, a point along a line of symmetry, the volume contribution is:

$$\Delta V \simeq \frac{1}{2} \phi_3 \ (h \cdot k) \tag{17}$$

If the region were composed of only Type 1 and Type 3 points this method of computing the volume is an application of the trapazoidal rule. However, the presence of Type 2 and/or Type 4 points requires some special considerations.

Consider the Type 2 point adjacent to a Type 1 point shown in Fig. 4-A. According to the trapazoidal rule as applied using Eqs. 16 and 17 the volume contribution is zero because $\phi = 0.0$ at Type 2 points. However, it is known that the stress function always has the same algebraic sign. Therefore, for this application, an improvement on the volume calculations could be made by including the triangular prism cross hatched in Fig. 4-A. The volume contribution could be approximated as:

$$\Delta V \simeq \frac{1}{8} \phi_i \ (h \cdot k) \tag{18}$$

This same volume contribution is used when Type 2 points lie on a sloping edge. Due to the coding of the integration routine this correction could be applied twice in the case of a Type 2 point on a sloping edge which would create an overestimation of the volume.

The reasons why this overestimation is quite small are as follows:

1. In the approximately 75 times this program has been executed Type 2 points have fallen on a sloping edge only twice by chance selection of a mesh size. Furthermore, it is always possible to avoid this situation, if desired, by careful discretization.

2. The value of the stress function used is always one of the smaller values due to the proximity to the free edge.

3. The area involved is usually one-half of the area used for an interior point.

4. The large number of points used here makes the volume contribution of each point a small part of the total. This is especially true for edge points as mentioned in No. 3.

A type 4 point in a corner for which both sides of the boundary are adjacent to the mesh lines is shown in Fig. 4-B. The volume contribution could be approximated as:

$$\Delta V \simeq \phi 4 \left[\frac{3}{4} h \cdot k + \frac{1}{6} h_1 \cdot k_1\right] \quad \begin{matrix} h_1 < \frac{h}{2} \\ k_1 < \frac{k}{2} \end{matrix} \tag{19}$$

This equation is quite approximate but the point shown in Fig. 4-B occurs at most only once as shown and once with $k_1 = k/2$. In this latter case Eq. 19 is less approximate.

A Type 4 point in which only one side is adjacent to the mesh line is shown in Fig. 4-C. The volume contribution is approximated by either equation below.

$$\Delta V \simeq \phi 4 \ [\frac{1}{2}\, h \cdot k + \frac{1}{2}\, h_1 \cdot k] \tag{20}$$

$$\Delta V \simeq \phi 4 \ [\frac{1}{2}\, h \cdot k + \frac{1}{2}\, h \cdot k_1]$$

Eq. 20 is used for the Type 4 points on the left side of Fig. 4-C while Eq. 21 is used for Type 4 points on the bottom of the flange.

A Type 4 point adjacent to a sloping edge is treated in one of three ways:

$$\Delta V \simeq \phi 4 \ [\frac{3}{4}\, h \cdot k + \frac{1}{6}\, h_1 \cdot k], \qquad h_1 < \frac{h}{2} \tag{22}$$

$$\Delta V \simeq \phi 4 \ [\frac{3}{4}\, h \cdot k + \frac{1}{6}\, h \cdot k_1], \qquad k < \frac{k}{2} \tag{23}$$

$$\Delta V \simeq \phi 4 \ [\frac{3}{4}\, h \cdot k + \frac{1}{6}\, h_1 \cdot k_1], \qquad h_1 < \frac{h}{2}, \quad k_1 < \frac{k}{2} \tag{19}$$

These three cases are shown in Fig. 4-D.

While more sophisticated ways could be developed to handle points along the sloping edge it is believed that, for the four reasons enumerated earlier in this section, the methods used here are adequate.

2.2 Applications of Approximate Equations

Equations 5, 6 and 7 were used as four of the six approximate ways to compute approximate torsional constants, as stated in Chapter 1, Eqs. 5 and 6 apply to rectangular sections. It was therefore necessary to convert the I-shapes into an assemblage of rectangles. This was done by defining t_1 as the thickness of a rectangle corresponding to the portion of the I-shape above the junction of the web and the top sloping flanges as shown in Fig. 1. t_2 is a corresponding thickness for the lower portion of the I-shape. The third rectangle, corresponding to the web had the dimensions d_3 and b_3 as shown in Fig. 1. t_1 and t_2 are defined by the equations below using the notation of Fig. 1:

$$t_1 = d_1 + \frac{d_2 (b_1 + b_3)}{2 b_1} \tag{24-A}$$

$$t_2 = d_5 + \frac{d_4 (b_3 + b_2)}{b_2} \tag{24-B}$$

This division of areas results in the idealized shape shown in Fig. 1-B. The torsional constant was computed as the sum of the torsional constants of the three rectangles using Eqs. 5-A and 6-A below.

$$K_T = \frac{1}{3} \sum_{i=1}^{3} b_i t_i^3 \left[1.0 - 0.63 \frac{t_i}{b_i} + 0.052 \left(\frac{t_i}{b_i} \right)^2 \right] \tag{5-A}$$

$$K_T = \frac{1}{3} \sum_{i=1}^{3} b_i t_i^3 \tag{6-A}$$

The dimensions t_i and b_i are as defined in Section 1.2. Eq. 5-A includes an approximate end slope correction but does not include the junction correction. Eq. 6-A was included in this presentation because, as stated in Ref. 5, the end slope reduction and the junction increase tend to offset each other when evaluating the torsional constant for a section which is idealized as being built up of individual rectangles and/or trapazoids.

Equation 7 was also applied to the idealized section shown in Fig. 1-B as shown in Eq. 7-A.

$$K_T = \sum_{i=1}^{3} \frac{A_i^4}{40\, I_{pi}} \qquad (7\text{-A})$$

It is noted that there are no reentrant corners in the idealization. Reference 7 indicates that Eq. 7 can over or underestimate the torsional constant for a rectangle by as much as 10% depending on the ratios of the sides. Summation of individual values of K_T using Eq. 7-A also neglects the junction stiffening of connected rectangles and should produce a low estimate of K_T for the complete section.

Equation 7-A was also applied to the idealization shown in Fig. 1-C. Junction stiffening was neglected in this case too.

Equations 9, 10 and 11 were also applied to the idealization shown in Fig. 1-B as the fifth approximate method. It was assumed that the end slope correction for each flange can be added in separately as one-half of the total end slope correction which would be computed for a doubly symmetric section. Two values of D_1 and α_1 will be computed on the same basis to compute two junction corrections. The fillet radius, r, will be assumed to be zero. Thus Eqs. 9, 10 and 11 can be rewritten as 9-A, 10-A and 11-A. t_1 and t_2 will be computed using Eq. 24 and the notation in Fig. 1-B.

$$K_T = \frac{1}{3}\left(b_1 t_1^3 + b_2 t_2^3 + d_3 t_3^3\right) + \alpha_1 D_1^4 + \alpha_2 D_2^4 - 0.21\left(t_1^4 + t_2^4\right) \qquad (9\text{-A})$$

$$D_1 = t_1 + \frac{b_3^2}{4\,t_1}$$

$$D_2 = t_2 + \frac{b_3^2}{4\,t_2} \qquad (10\text{-A})$$

$$\alpha_1 = -0.042 + 0.2204\,\frac{b_3}{t_1} - 0.0725\left(\frac{b_3}{t_1}\right)^2$$

$$\alpha_2 = -0.042 + 0.2204\,\frac{b_3}{t_2} - 0.0725\left(\frac{b_3}{t_2}\right)^2 \qquad (11\text{-A})$$

It has been assumed that the t's in Eq. 9-A are the smaller of each pair of dimensions. Thus t_3 is usually b_3 in Fig. 1-B.

The sixth approximate method of computing K_T was to equate K_T to the polar moment of inertia. This is the least desirable method investigated.

3. PRESENTATION OF RESULTS

3.1 Verification of Finite Difference Results

Seven test examples for which solutions were available were used to test the computer program which performed the finite difference analysis. These examples included a square, three rectangles, an equilateral triangle and two hypothetic I-beams to which the equations of El-Darwish and Johnston could be applied (Ref. 5). These equations were quite similar to the earlier work by Lyse and Johnston and were therefore considered verified (Ref. 8). The previous work on AASHO sections was not used as test examples because no corroberating evidence was found for these results.

3.1.1 Comparison with Theoretical Solution for a Square

Table III shows various results obtained for a square using different numbers of points. As the number of points increases the value of K_T rapidly approaches the theoretically exact value of 2.250 a_4 where "a" is a half-side (Ref. 11). The finite difference result of 2.235 a_4 is 0.67% low.

3.1.2 Comparison with Theoretical Solutions for Rectangles

Results for three rectangles with ratios of depth to width of 2.0, 3.0 and 4.0 are shown in Table III. "a" and "b" are half-sides with b > a. The corresponding absolute valued percent errors are 1.14%, 0.59% and 0.16%.

3.1.3 Comparison with Theoretical Result for an Equilateral Triangle

Table III shows a comparison of finite difference and theoretical values of K_T for an equilateral triangle. The sides were 10 inches long. The finite difference result is 0.74% low.

3.1.4 Comparisons with Two Hypothetical I-Beams

Two hypothetical, doubly symmetric I-beams were also investigated. Each was composed of three rectangles of equal dimensions. The dimension "b" shown in Fig. 5 was 18 inches. The minor dimension of the component rectangles was 6 inches and 3 inches respectively. The accepted values of K_T for these sections were computed using equations in Ref. 5. These results and the finite difference solutions are shown in Table III. For the thinner I-beam there is 1.42% difference; for the stockier section there is 0.45% difference.

3.2 Presentation of Results for Twenty-Five Sections

Table IV shows the finite difference results obtained for the twenty-five sections investigated. Values for the St. Venant torsional constant and torsional shear stress coefficients are shown. The values shown in Table IV agree reasonably well with the previous values in Table II except for the Type III beam. In that case there is about 11.5% difference in the values of K_T.

Each beam in Table IV has been analyzed using at least two finite difference meshes. The first mesh was square and was chosen to put as many points as possible in the mesh using the existing program. Between 160 and 185 points for which $\phi \neq 0.0$ were used in each mesh. These meshes typically had Type 2 points on only one side parallel to a major or minor axis. Consideration of the integration scheme and observation of the test examples indicated that it was generally slightly more accurate to develop a mesh which had Type 2 points on all sides parallel to the major and minor axes. Rectangular meshes were developed which did this. All but one of the values in Table IV resulted from these rectangular meshes. There was an average difference between the two types of meshes of only 1.75%. The larger values are shown in Table IV.

The AASHO Type III section was analyzed with six different meshes using between 119 and 173 points. Both square and rectangular meshes were used. There was 1.97% difference between the largest and smallest values.

The shear stress coefficients have been calculated using equations presented by Tamberg (Ref. 9). The shear stress at the midpoint of the edges of the top and bottom flanges and near the midpoint of the edge of the web are given by Eq. 25.

$$\tau = \beta G \phi' \tag{25}$$

β is the corresponding stress coefficient in Table IV.

Table V contains values of the ratio $\frac{GK_T}{EI}$ for the Poisson's ratio equal to 0.15 and 0.20. It is these values which are used in the lateral load distribution study mentioned in Chapter 1.

Table VI contains the results of applying the various approximate methods for computing K_T to 23 of the 25 sections. The AASHO Type V and VI beams were not included because these shapes were idealized to fit the shape shown in Fig. 1-A. Figure 6 shows values of "percent of finite difference results" versus "beam number" for these 23 sections. Each part of Fig. 6 thus shows the agreement, or lack of agreement, between one of the six approximate methods and the finite difference results. Beam No. 1 is the AASHO Type I, Beam No. 4 is the AASHO Type IV, Beam No. 5 is the 18/30 and Beam No. 23 is the 26/63 section.

Figure 6-A shows that Eq. 5-A always underestimates because it includes only the end slope correction.

Figure 6-B shows that Eq. 6-A can either under or overestimate the finite difference value. This is because Eq. 6-A includes neither the end slope reduction or the junction addition.

Figures 6-C and D show that Eq. 7-A also underestimates K_T for both discretizations shown in Fig. 1-B and C. This is also because only the end slope correction was included.

Figure 6-E shows that using the polar moment of inertia always overpredicted by a large amount. In the worst case there was about 1100% error.

Figure 6-F shows that the modified method of El-Darwish and Johnston as explained in Section 2.2 yielded consistently excellent results. All of the approximate torsional constants computed in this manner were within ±5% of their respective finite difference value.

4. SUMMARY AND CONCLUSIONS

This research has presented and compared St. Venant torsional constants for twenty-five prestressed concrete bridge beams using seven different techniques. The results computed by finite differences are thought to be the most accurate values.

The finite difference computer program was tested using seven example problems. Excellent agreement with accepted solutions was noted.

Torsional shear stress coefficients computed from the finite difference results were also presented for the twenty-five beams.

A comparison of the six approximate methods of computing K_T versus the finite difference results was also presented. From these comparisons it was noted that the modified method of El-Darwish and Johnston provided consistently excellent approximations. Equating the torsional constant to the polar moment of inertia was the worst approximation investigated. The other four methods gave intermediate results.

5. TABLES

TABLE 1: DIMENSIONS OF I-BEAMS (INCHES)

Name	D1	D2	D3	D4	D5	B1	B2	B3
Type I	4	3	11	5	5	12	16	6
Type II	6	3	15	6	6	12	18	6
Type III	7	4½	19	7½	7	16	22	7
Type IV	8	6	23	9	8	20	26	8
Type V*	5	3	37	10	8	42	28	8
Type VI*	5	3	46	10	8	42	28	8
18/30	3	3	12	8	4	12	18	6
20/30	3	3	12	8	4	14	20	8
18/33	4	3	12	8	6	12	18	6
20/33	4	3	12	8	6	14	20	8
24/33	4	3	12	8	6	18	24	12
26/33	4	3	12	8	6	20	26	14
18/36	5	3	12	8	8	12	18	6
20/36	5	3	12	8	8	14	20	8
24/36	5	3	12	8	8	18	24	12
26/36	5	3	12	8	8	20	26	14
20/39	8	3	12	8	8	14	20	8
24/42	4	4	17	10	7	18	24	8
24/45	7	4	17	10	7	18	24	8
24/48	8	4	17	10	9	18	24	8
24/51	11	4	17	10	9	18	24	8
24/54	14	4	17	10	9	18	24	8
24/60	6	6	29	10	9	24	24	8
26/60	6	6	29	10	9	26	26	10
26/63	9	6	29	10	9	26	26	10

* Idealized Dimensions Used in This Study

TABLE II: PREVIOUS FINITE DIFFERENCE RESULTS FOR FOUR AASHO SECTIONS

Beam	No. of Points	K_T	τ_b	τ_t	τ_w
I	35	4,900 in^4.	8.4 $G\phi'$	5.9 $G\phi'$	6.3 $G\phi'$
II	40	8,300	9.9	7.7	6.2
III	35	19,000	12.3	9.8	7.6
IV	40	34,500	13.7	11.4	8.2

TABLE III: RESULTS FOR TEST EXAMPLES

Type of Example	K_T	No. of Points	Accepted Solution
Square	1.353 a^4	3	2.250 a^4
Square	2.070	6	2.250
Square	2.165	18	2.250
Square	2.193	45	2.250
Square	2.220	84	2.250
Square	2.221	110	2.250
Square	2.235	180	2.250
Rectangle (2:1)	3.622 a^3b	168	3.664 a^3b
Rectangle (3:1)	4.183	---	4.208
Rectangle (4:1)	4.503	---	4.496
Equilateral Triangle	214.9 in^4.	---	216.5 in^4.
I-BM (6:1)	487.0	162	494.0
I-BM (3:1)	4,003.0	180	4,021.0

TABLE IV: FINITE DIFFERENCE RESULTS

Beam	No. of Points	K_T in.^{4}	τ_b $G\phi'$	τ_t $G\phi'$	τ_w $G\phi'$
Type I	133	4,745	8.59	6.84	6.17
Type II	177	7,793	9.69	7.51	6.10
Type III	150	17,044	11.52	9.46	7.14
Type IV	122	32,924	13.52	11.35	8.10
Type V	147	35,433	14.33	9.63	8.00
Type VI	162	36,071	14.23	9.63	8.00
18/30	121	5,818	12.68	6.18	5.95
20/30	145	9,142	14.57	7.11	8.28
18/33	128	8,418	13.99	6.84	6.17
20/33	133	12,474	11.04	7.78	9.35
24/33	136	25,576	21.01	10.05	12.31
26/33	162	33,942	13.84	11.31	14.10
18/36	161	11,310	15.39	7.24	6.17
20/36	170	16,119	11.86	8.09	8.55
24/36	167	32,034	22.76	10.35	12.76
26/36	165	42,365	14.79	11.70	14.48
24/39	165	18,723	11.96	9.17	8.65
24/42	139	21,864	12.87	8.46	8.32
24/45	134	25,007	12.90	10.13	8.38
24/48	169	31,295	13.83	10.51	8.35
24/51	153	35,137	13.91	11.55	8.27
24/54	158	39,648	13.86	12.03	8.27
24/60	166	35,165	17.43	11.07	7.73
26/60	156	48,005	19.42	11.78	10.04
26/63	136	55,207	14.72	13.49	10.16

TABLE V: VALUES OF $\frac{GK}{EI}$

Beam	I	K_T (F.D.)	$\frac{GK}{EI}$ (μ = .15)	$\frac{GK}{EI}$ (μ = .20)
Type I	22,750	4,745	0.0907	0.0869
Type II	50,980	7,793	0.0665	0.0637
Type III	125,390	17,044	0.0591	0.0566
Type IV	260,730	32,924	0.0549	0.0526
Type V	521,163	35,433	0.0296	0.0283
Type VI	733,320	36,071	0.0214	0.0205
18/30	27,840	5,818	0.0909	0.0871
20/30	32,596	9,142	0.1219	0.1169
18/33	38,336	8,418	0.0955	0.0915
20/33	44,514	12,474	0.1218	0.1168
24/33	57,195	25,576	0.1944	0.1863
26/33	63,340	33,942	0.2330	0.2233
18/36	50,729	11,310	0.0969	0.0929
20/36	58,976	16,119	0.1188	0.1139
24/36	75,253	32,034	0.1851	0.1774
26/36	83,324	42,365	0.2211	0.2118
20/39	77,514	18,723	0.1050	0.1006
24/42	107,986	21,864	0.0880	0.0844
24/45	140,129	25,007	0.0776	0.0744
24/48	172,692	31,295	0.0788	0.0755
24/51	212,450	35,137	0.0719	0.0689
24/54	255,194	39,648	0.0675	0.0647
24/60	354,888	35,165	0.0431	0.0413
26/60	391,487	48,005	0.0533	0.0511
26/63	470,081	55,207	0.0511	0.0489

TABLE VI: RESULTS OF APPROXIMATE METHODS

Equation	7-A	7-A	5-A	6-A	9-A
Figure	1-B	1-C	1-B	1-B	1-B
Beam	$\frac{A_i^4}{40 I_{po}}$		$\frac{bt^3}{3} - Ad^3$	$\frac{bt^3}{3}$	
Type I	3,497	3,770	3,388	4,972	4,584
Type II	6,337	6,750	6,142	9,326	7,762
Type III	14,057	15,053	13,630	20,382	16,845
Type IV	27,337	29,402	26,515	39,229	32,265
18/30	4,519	4,988	4,381	6,321	5,623
20/30	6,154	6,841	5,970	8,664	8,787
18/33	6,943	7,356	6,723	10,575	8,325
20/33	9,179	9,861	8,890	13,653	12,398
24/33	14,376	15,621	13,850	22,384	25,490
26/33	17,199	18,717	16,669	25,497	32,260
18/36	9,892	10,199	9,567	16,610	11,510
20/36	12,907	13,522	12,494	20,676	16,783
24/36	19,792	21,086	19,080	31,395	32,587
26/36	23,505	25,141	22,750	35,507	41,077
20/39	14,612	15,236	14,140	24,002	19,089
24/42	17,556	18,997	17,017	25,284	21,335
24/45	20,028	21,534	19,399	29,125	24,362
24/48	26,655	28,018	25,809	41,410	31,696
24/51	30,620	31,976	29,626	49,739	36,395
24/54	35,386	36,703	34,009	62,567	41,505
24/60	29,688	31,569	28,874	43,712	34,558
26/60	37,761	40,377	36,711	53,729	47,001
26/63	44,811	47,637	43,499	64,380	55,242

6. FIGURES

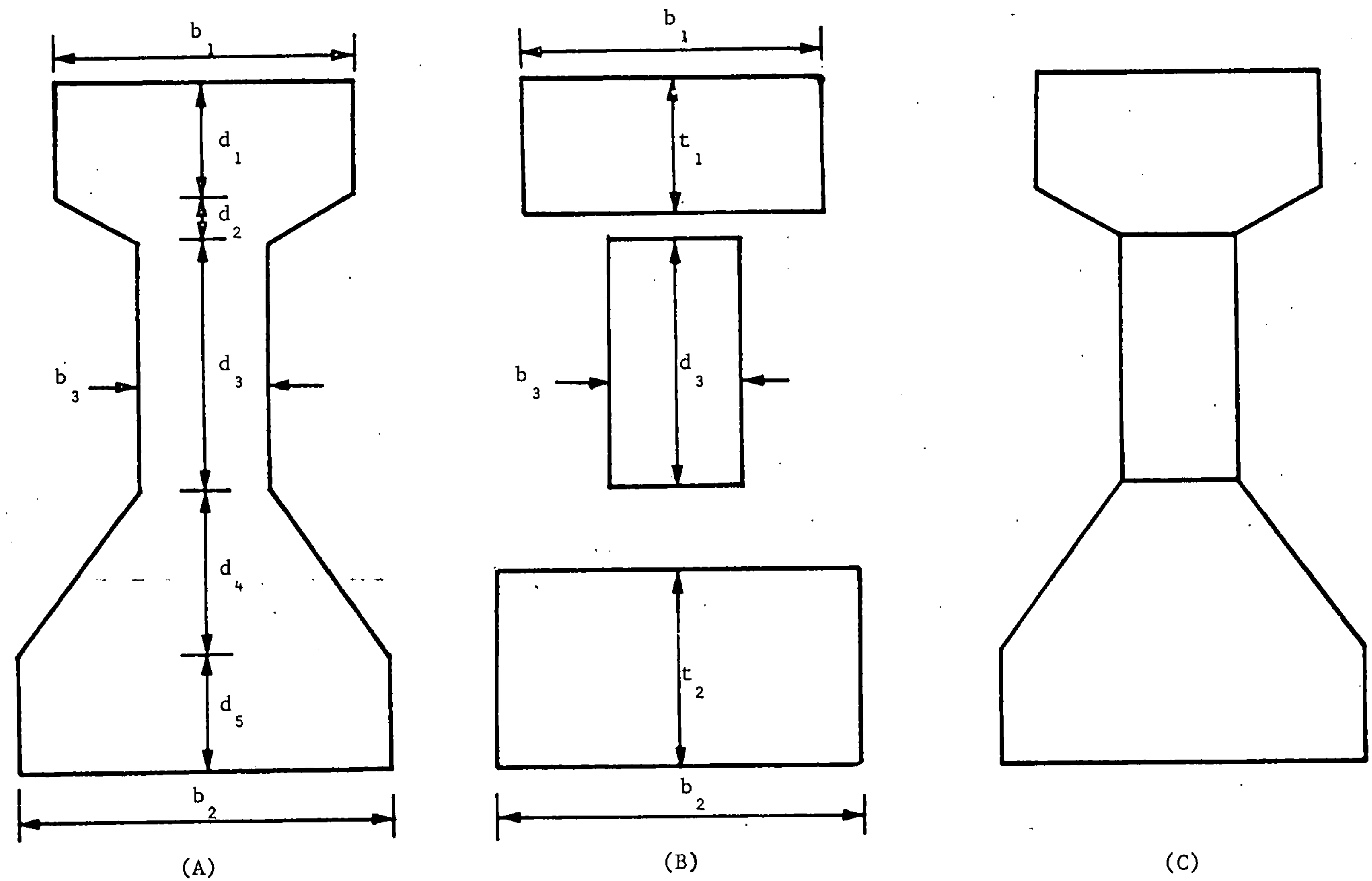

Fig. 1 General I-Beam and Discretizations

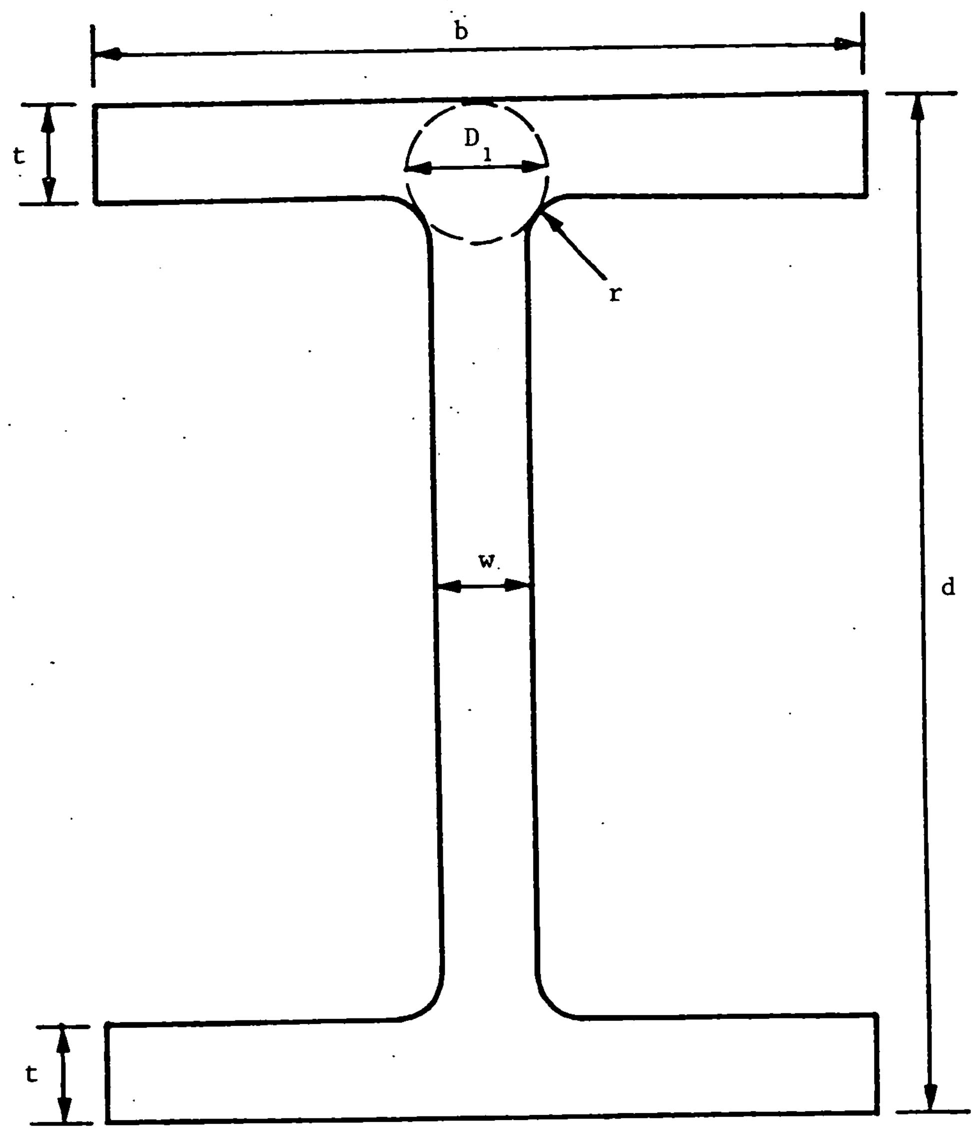

Fig. 2 Doubly Symmetric I-Beam

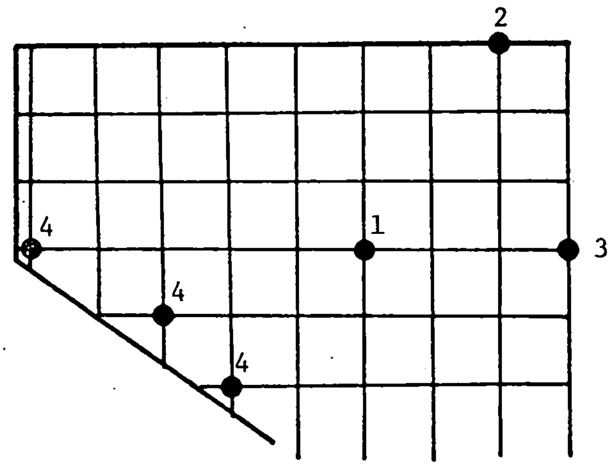

Fig. 3-A Types of Mesh Points

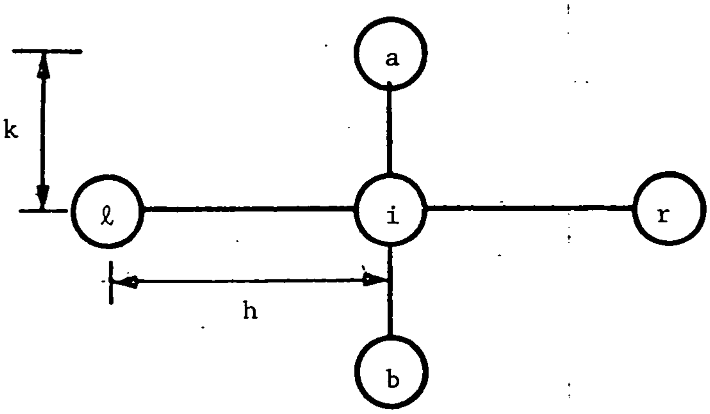

Fig. 3-B Finite Difference Operator

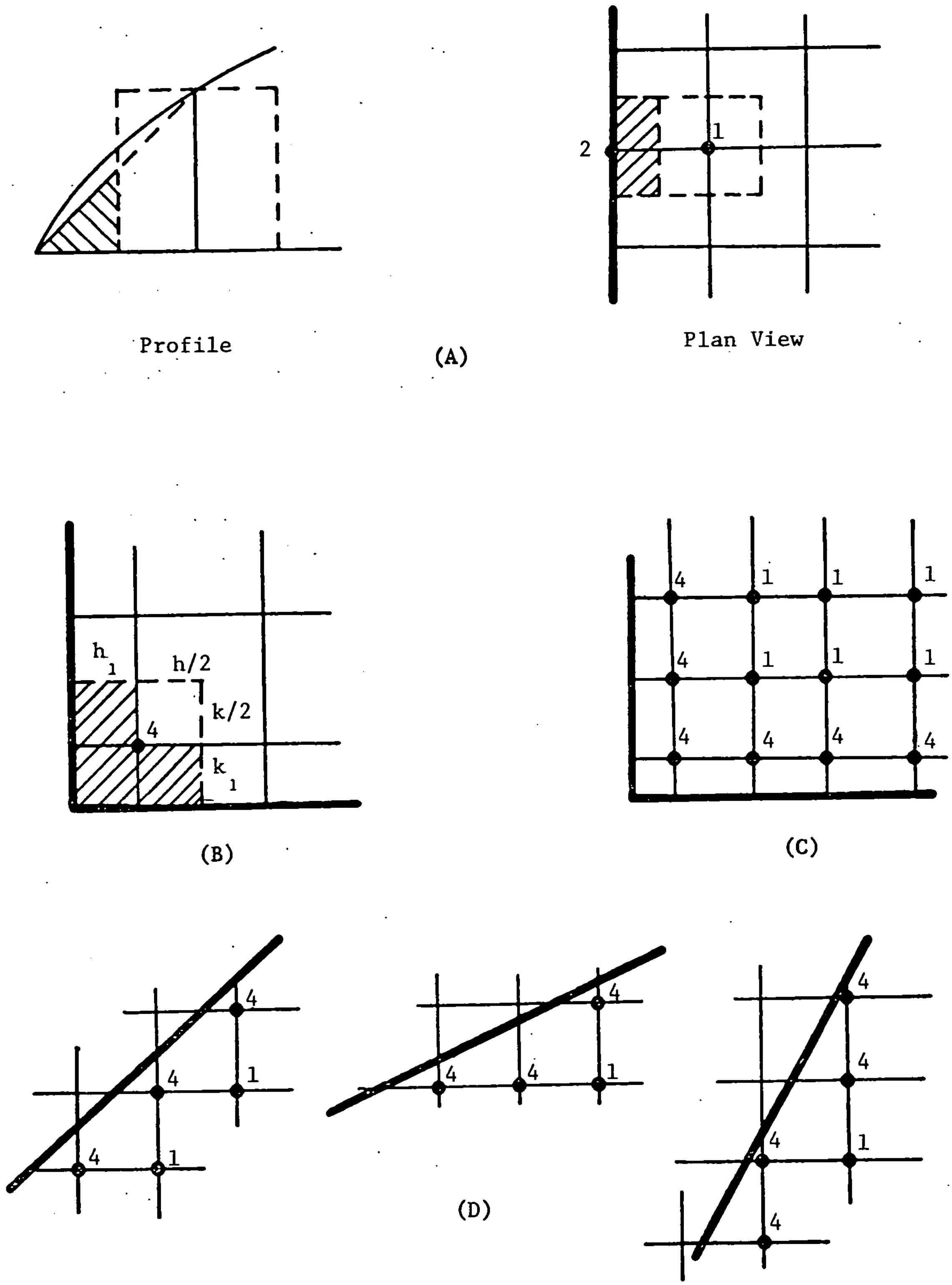

Fig. 4 Special Points for Integration

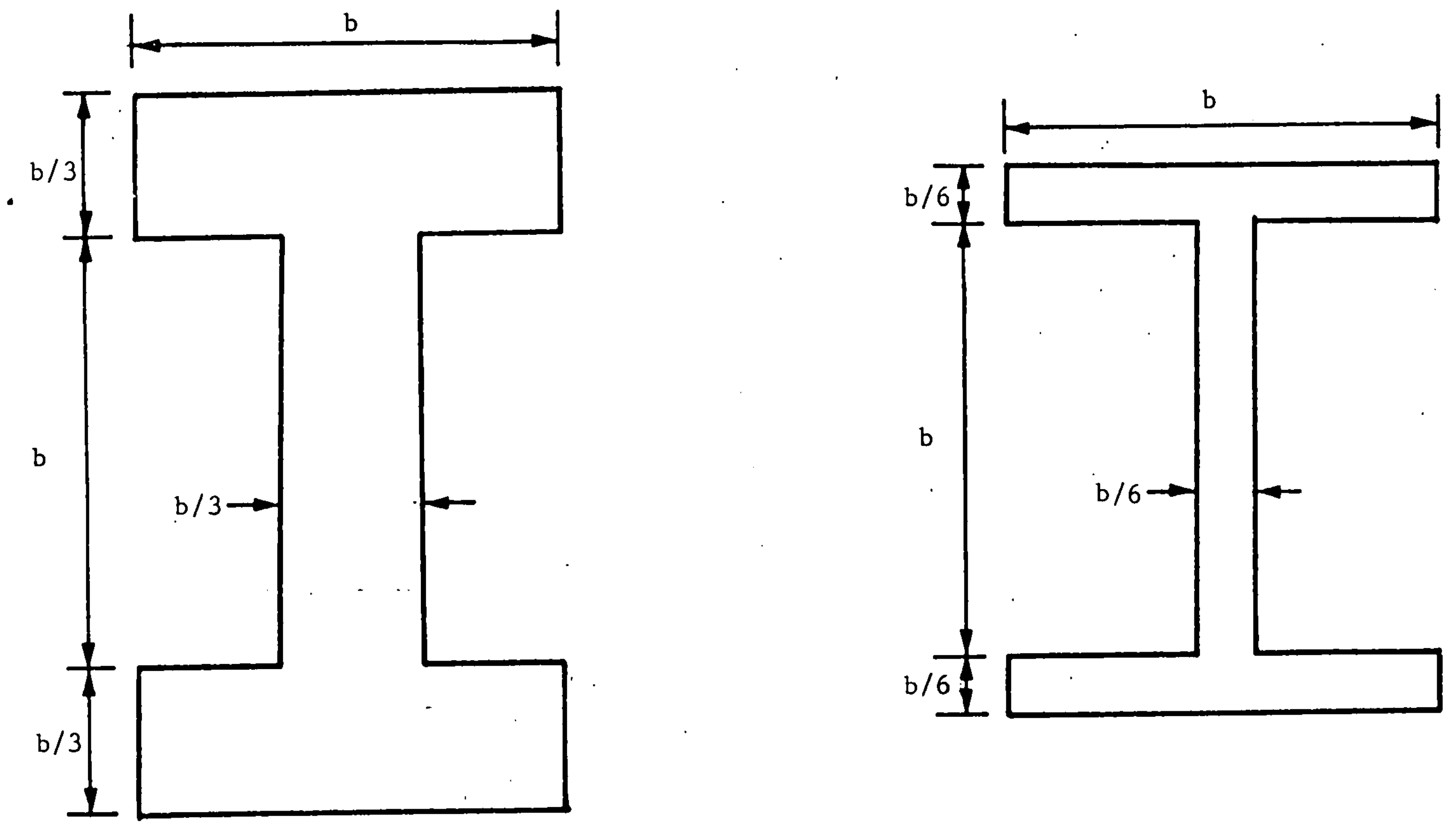

Fig. 5 Hypothetical I-Beams

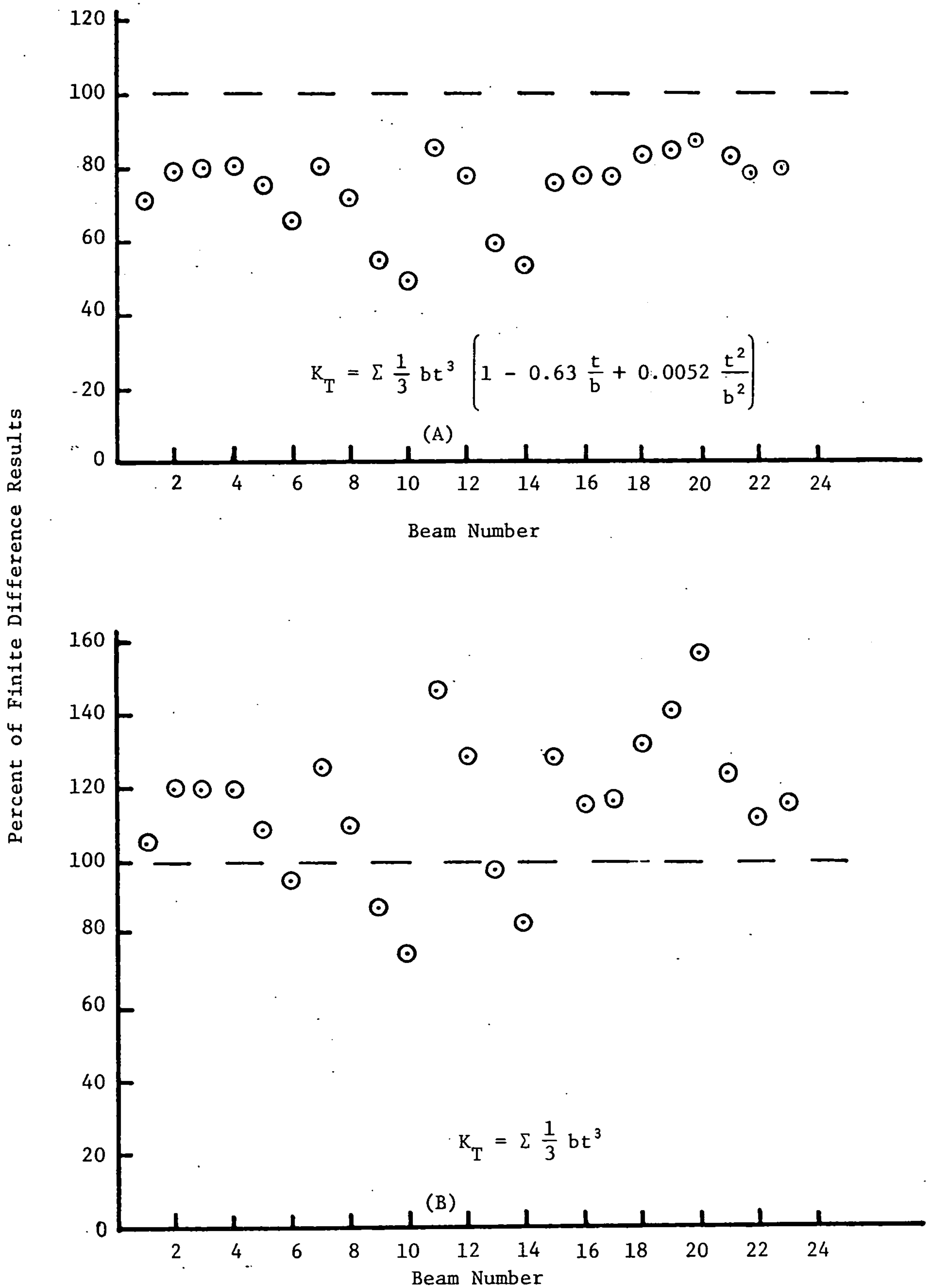

Fig. 6 Comparison of Approximate and Finite Difference Results

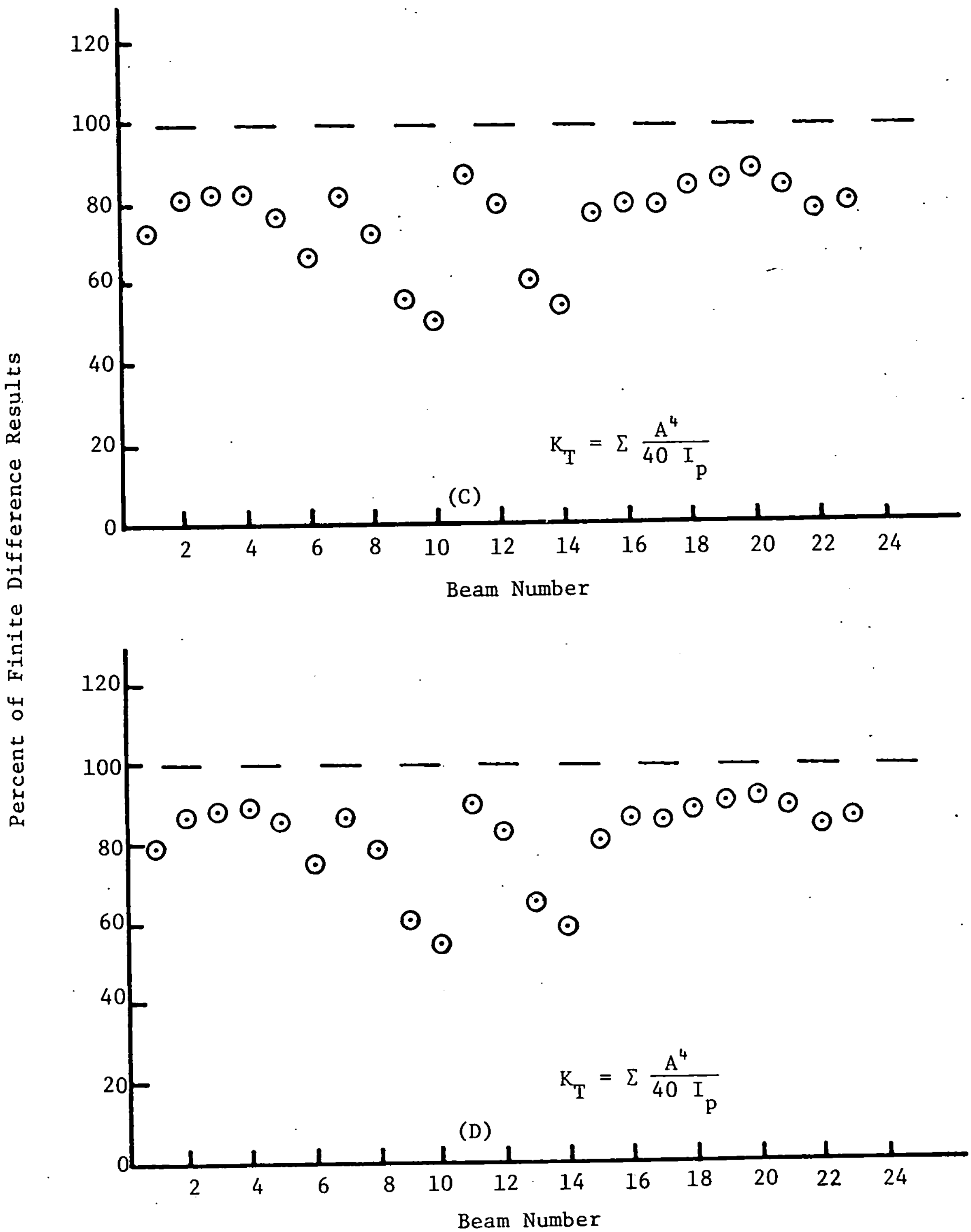

Fig. 6 (Continued)

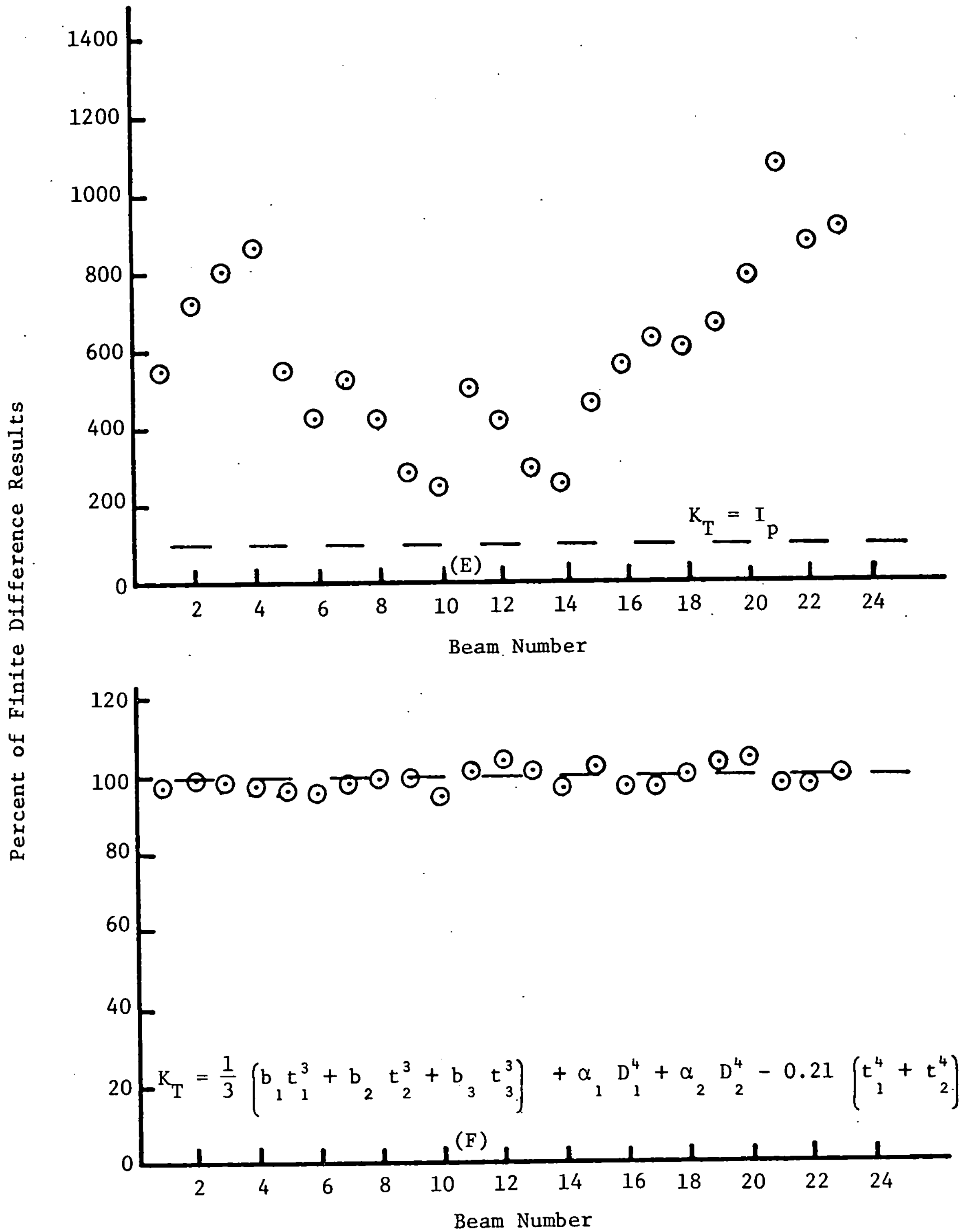

Fig. 6 (Continued)

7. REFERENCES

1. ALCOA STRUCTURAL HANDBOOK, Aluminum Company of America, Pittsburgh, Pennsylvania, 1960.

2. STANDARDS FOR BRIDGE DESIGN (PRESTRESSED CONCRETE STRUCTURES), BD201, Pennsylvania Department of Transportation, Harrisburg, Pennsylvania, 1973.

3. STANDARDS FOR PRESTRESSED CONCRETE BRIDGES, ST208, Pennsylvania Department of Transportation, Harrisburg, Pennsylvania, 1964.

4. DeCastro, E. S. and Kostem, C. N.
USER'S GUIDE - COMPUTER PROGRAM FOR THE ANALYSIS OF ECCENTRICALLY STIFFENED PLATES, Under preparation.

5. El-Darwish, I. A. and Johnston, B. G.
TORSION OF STRUCTURAL SHAPES, Journal of Structural Division, Proceedings of ASCE, Vol. 91, No. ST1, February 1965.

6. Galambos, T. V.
STRUCTURAL NUMBERS AND FRAMES, Prentice Hall, 1968.

7. Kollbrunner, C. F. and Basler, K.
TORSION IN STRUCTURES, Springer-Verlag, New York, 1969.

8. Lyse, I. and Johnston, B. G.
STRUCTURAL BEAMS IN TORSION, Transactions ASCE, Vol. 101, p. 857, 1936.

9. Tamberg, K. G.
ELASTIC TORSIONAL STIFFNESS OF PRESTRESSED CONCRETE AASHO GIRDERS, an ACI two-part paper, ACI Journal, April 1965.

10. Trayer, G. W. and March, H. W.
THE TORSION OF MEMBERS HAVING SECTIONS COMMON IN AIRCRAFT CONSTRUCTION, Technical Report to the Advisory Committee for Aeronatutics, No. 334, 1930.

11. Wang, C. T.
APPLIED ELASTICITY, McGraw-Hill, 1953.

12. Wegmuller, A. W.
FINITE ELEMENT ANALYSIS OF ELASTIC-PLASTIC PLATES AND ECCENTRICALLY STIFFENED PLATES, Ph.D. Dissertation, Civil Engineering Department, Lehigh University, 1971.

13. Zellin, M. A., Kostem, C. N. and VanHorn, D. A.
STRUCTURAL BEHAVIOR OF BEAM-SLAB HIGHWAY BRIDGES - A SUMMARY OF COMPLETED RESEARCH AND BIBLIOGRAPHY, Fritz Engineering Laboratory Report No. 387.1, Lehigh University, May 1973.

8. APPENDICES

APPENDIX A

USER'S GUIDE TO PROGRAM "TORSION"

Program TORSION performs the finite difference analysis discussed in this report to evaluate the St. Venant torsional constant for a shape like that shown in Fig. A-1. Degenerate shapes may also be analyzed if they are symmetric about at least one axis and provided that D3 and D7 shown in Fig. A-1 are not zero.

A.1 Input

First Card: A label of up to ten alphanumeric characters. Format A10.

Second Card: D1, D2, D3, D4, D5, D6, D7 and D8 as shown in Fig. A-1. Format 8F10.0.

Third Card: D9, grid dimension "h", grid dimension "k". Format 8F10.0.

Fourth Card: The ratio k/h.

Fifth Card: CODE 1, the minimum number of mesh points desired, the maximum number of mesh points desired. Format A3, 2F10.0.

If CODE 1 = yes, the original grid dimensions on the third card will be the only ones tried. If CODE 1 ≠ yes, an attempt will be made to find grid dimensions which produce a number of points which falls between the limits set on the fifth card. It is desirable to have CODE 1 ≠ yes so that any reasonable set of dimensions can be read in for the grid size. An error message is produced if a suitable mesh cannot be found from the starting mesh. Remedial action is to try another mesh size.

Sixth Card: CODE 2. Format A3.

If CODE 2 = yes the subtotals in the volume integration are printed out. The normal mode is Code 2 ≠ yes.

A.2 Output

Output usually consist of five items.

1. Echo print of input dimensions.
2. The grid dimensions used and the total number of Type 1, 3 and 4 points generated.
3. A plot showing the positions of Types 1, 2, 3 and 4 points in the cross-section.
4. A table of values of the stress function at each node point.
5. The value of the torsional constant.

If CODE 2 = yes the integration subtotals for each node will also be printed.

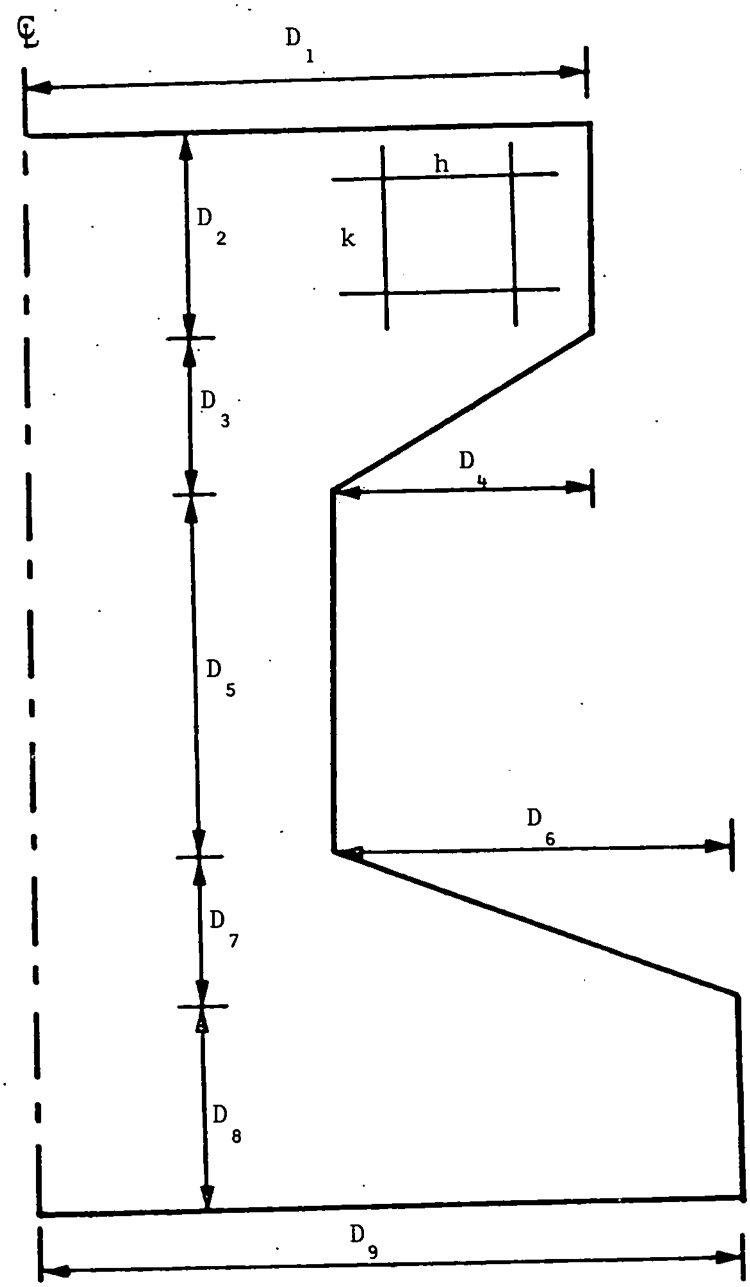

Fig. A-1 General Cross-Section

APPENDIX B

SOURCE PROGRAM LISTING

```
      PROGRAM ONE(INPUT,TAPE1=INPUT,OUTPUT=1,TAPE2=OUTPUT)
      INTEGER GP(30,90)
      COMMON /CE1/ GP,J,K,DIM,GRIDDEM,L,AK,JMAX,GRID,SQ,SQEM
      COMMON /CE2/ ANS(170),AR(170,170),KF,K1,N,K2(2)
      COMMON /CE3/ D2,DD2,D4,D3,B,DD3,DD4,D6,D7,BB,D9,D1,DD5
      WRITE (2,40)
      READ (1,41) LABEL
      READ (1,45) D1,D2,D3,D4,D5,D6,D7,D8,D9,GRIDDEM,GRID
      WRITE (2,42)
      WRITE (2,43) LABEL
      WRITE (2,46) D1,D2,D3,D4,D5,D6,D7,D8,D9
      WRITE (2,44)
      READ (1,47) BKB
      A=0.
1     L=0
      SQ=GRID*GRID
      SQEM=GRIDDEM*GRIDDEM
C       MAKE ALL POINTS OUTSIDE POINTS
      DO 2 K=1,90
      DO 2 J=1,30
      GP(J,K)=1H
2     CONTINUE
C       SUM DIMENSIONS
      DD2=D2+D3
      DD3=DD2+D5
      DD4=DD3+D7
      DD5=DD4+D8
      FOX=D1-D4+D6-D9
      IF (FOX.NE.0.) WRITE (2,48) FOX
C       TAKE CARE OF FIRST ROW AND COLUMN
      KIP=DD5/GRID+10
      LIP=D1/GRIDDEM+1
      IF (KIP.GT.90.OR.LIP.GT.30.) WRITE (2,49)
      IF (KIP.GT.90.OR.LIP.GT.30.) STOP
      DO 3 J=11,KIP
      L=L+1
      GP(1,J)=1H3
3     CONTINUE
      DO 4 J=1,LIP
      GP(J,10)=1H2
4     CONTINUE
C       SET COUNTERS
      JMAX=0
      AK=GRID
      K=1
      J=LIP
C       D2 SECTION
      DIM=D1/GRIDDEM
5     IF (AK.LE.D2) 6,7
6     CALL PTGR
      GO TO 5
C       D3 SECTION
7     B=D1+D2/D3*D4
8     Y=-D4/D3*(AK)+B
      DIM=Y/GRIDDEM
      J=Y/GRIDDEM+1
      IF (AK.LE.DD2) 9,10
9     CALL PTGR
      GO TO 8
C       D5 SECTION
10    J=(D1-D4)/GRIDDEM+1
      DIM=(D1-D4)/GRIDDEM
11    IF (AK.LE.DD3) 12,13
```

```
12    CALL PTGR
      GO TO 11
C       D7 SECTION
13    BB=(D1-D4)-DD3/D7*D6
14    Y=D6/D7*(AK)+BB
      DIM=Y/GRIDDEM
      J=Y/GRIDDEM+1
      IF (AK.LE.DD4) 15,16
15    CALL PTGR
      GO TO 14
C       D8 SECTION
16    J=D9/GRIDDEM+1
      DIM=D9/GRIDDEM
17    IF (AK.LT.DD5) 18,19
18    CALL PTGR
      GO TO 17
C       CHECK TO SEE IF THE LAST COLUMN IS ON THE BOUNDARY
19    K1=K+10
      IF (AK.EQ.DD5) 20,22
20    IF (J.LT.2) GO TO 22
      DO 21 J1=1,J
      GP(J1,K1)=1H2
21    CONTINUE
22    IF (GP(1,K1).EQ.1H2) L=L-1
      IF (A.NE.0.) GO TO 23
      A=1.
      READ (1,50) NO1,LL,LU
      IF (NO1.EQ.3HYES) GO TO 27
      WRITE (2,51) LL,LU
23    IF (L.GE.LL.AND.L.LE.LU) 27,24
24    IF (A.EQ.1) WRITE (2,55) L,GRIDDEM,GRID
      IF (A.NE.1.) WRITE (2,52) L
      IF (A.GE.10) 25,26
25    WRITE (2,53)
      STOP
26    A=A+1
      FOK=LL
      IF (L.GT.LU) FOK=LU
      GRIDDEM=GRIDDEM*L/FOK
      GRID=GRIDDEM*BKB
      WRITE (2,54) GRIDDEM,GRID
      GO TO 1
27    IF (A.EQ.1.) WRITE (2,54) GRIDDEM,GRID
      DO 30 J=2,JMAX
      K1=KIP
      DO 30 K=10,K1
      IF (GP(J,K).EQ.1H1) 28,30
28    IF (GP(J-1,K).EQ.1H ) GO TO 29
      IF (GP(J+1,K).EQ.1H ) GO TO 29
      IF (GP(J,K-1).EQ.1H ) GO TO 29
      IF (GP(J,K+1).EQ.1H ) GO TO 29
      GO TO 30
29    GP(J,K)=1H4
30    CONTINUE
      WRITE (2,52) L
C      WRITE OUT GRID
      WRITE (2,56)
      WRITE (2,57) ((GP(J,K),K=1,90),J=1,30)
C       SET COEFICIENT ARRAY TO ZERO
      DO 31 L=1,LU
      DO 31 M=1,LU
      AR(L,M)=0.
31    CONTINUE
C       SET NUMBER OF EQUATIONS TO ZERO
      N=0.
C       WRITE AN EQUATION FOR EACH VALID POINT
```

```
      DO 32 J=1,JMAX
      DO 32 KF=10,K1
      IF (GP(J,KF).EQ.1H .OP.GP(J,KF).EQ.1H2) GO TO 32
      CALL GETK2
      N=N+1
      IF (GP(J,KF).EQ.1H1) CALL TYPE1
      IF (GP(J,KF).EQ.1H3) CALL TYPE3
      IF (GP(J,KF).EQ.1H4) CALL TYPE4
32    CONTINUE
      READ (1,58) NQUES
      IF (NQUES.EQ.3HYES) 33,35
33    DO 34 JL=1,N
      WRITE (2,59) (AR(JL,KL),KL=1,N),ANS(JL)
34    CONTINUE
C       CALL FLMXPK TO SOLVF THE SIMULTANEOUS EQUATIONS
35    CALL SOLV1 (AR,ANS,N,1,DET)
      WPITE (2,60)
      N=1
      DO 39 J=1,JMAX
      I=9
      DO 38 K=10,K1
      I=I+1
      IF (GP(J,K).EQ.1H .OR.GP(J,K).FQ.1H2) 36,37
36    AR(I,1)=0.
      GO TO 38
37    AP(I,1)=ANS(N)
      N=N+1
38    CONTINUE
      WRITE (2,61) (AR(I,1),I=10,K1)
39    CONTINUE
      CALL IRT
      STOP
C
40    FORMAT (1H1)
41    FORMAT (A10)
42    FORMAT (//////,10X,* THIS FROGRAM SOLVES FOR TORSIONAL*,/,10X,* CO
     1NSTANTS OF BEAMS BY A FINITE*,/,10X,* DIFFERENCE ANALYSIS*,//)
43    FORMAT (/,6X,A10)
44    FORMAT (10X,*     D2       D3            D7     D8           *,/
     1,10X,*  ..........                    .........      *,/,10X,*
     2.         .                 .         .         *,/,10X,*  .
     3      .               .         .        *,/,10X,*  .
     4.  D4      D6  .          .         *,/,10X,*  .           .
     5        .           .       *,/,10X,*D1.             .   D5
     6.             .      *,/,10X,*  .              ..........
     7      . D9   *,/,10X,*  .                                    .
     8  *,/,10X,*  .                                     .       *,/,10
     9X,*  .                                     .        *,/,10X,*  ..
     $.....................................        *,/,10X)
45    FORMAT (8F10.5,/,3F10.5)
46    FORMAT (4X,*BEAM DIMENSICNS*,/,4X,*D1*,4X,*D2*,4X,*D3*,4X,*D4*,4X,
     1*D5*,4X,*D6*,4X,*D7*,4X,*D8*,4X,*D9*,/9F6.2//)
47    FORMAT (F10.2)
48    FORMAT (/,10X,*THE BEAM MUST BE SYMETRIC *,/,10X,*ABOUT THE Y-AXIS
     1  ERROR= *,E14.7)
49    FORMAT (///,11X,*IF A MODE =1 ERROR HAS DEVELOPED*,/,10X,* IT IS D
     1UE TO THE FACT THAT THE FROGRAM*,/,10X* WAS DEVELOPED FO**R CONCRE
     2TE BEAMS AND*,/,10X*THIS BEAM IS TOO SLENDER -----*,/,10X,* CORREC
     3T , CHANGE GRID DIMENSIONS*)
50    FORMAT (A3,2X,I3,2X,I3)
51    FORMAT (//,10X,*THE PROGRAM IS FINDING A GRID VALUE*,/,10X,*WHICH
     1LIMITS THE NUMBER OF EQUATIONS BETWEEN *I3,* AND *,I3/)
52    FORMAT (4X,*NUMBER OF GRID POINTS*,4X,I3,////)
53    FORMAT (10X,* THE NUMBER OF GRID POINTS IS NOT CONVERGING*)
54    FORMAT (4X,*GRID DIMENSION*,2X,F6.4,* +X*,F6.4,*+*)
55    FORMAT (4X,*NUMBER OF GRID POINTS*,4X,I3,/,4X,*GRID DIMENSION*,2X,
```

```
     1F6.4,*+ X*,F6.4*,*////)
 56   FORMAT (5X,*IN THE GRID BELOW-1 IS AN INSIDE POINT*,/,23X,*2 IS A
     1BORDER POINT*,/,23X,*3 IS A DOUBLE POINT*,/,23X,*4 IS A POINT WHIC
     2H IS NEXT  TO THE BORDER *,///)
 57   FORMAT (90A1)
 58   FORMAT (A3)
 59   FORMAT (30F4.1)
 60   FORMAT (11X,*GIVEN BELOW ARE THE HEIGHT COORDINATES*/,10X,* OF THE
     1 ABOVE GRID*//)
 61   FORMAT (22F6.1)
      END
      SUBROUTINE IRT
      INTEGER GP(30,90)
      COMMON /CE1/ GP,J,K,DIM,GRIDDEM,L,AK,JMAX,GRID,SQ,SQEM
      COMMON /CE2/ ANS(170),AR(170,170),KF,K1,N,K2(2)
      COMMON /CE3/ D2,DD2,D4,D3,B,DD3,DD4,D6,D7,B8,D9,D1,DD5
      EXVOL=0.
      VOL=0.
      NN=K1-11
      IF (GP(2,K1).EQ.1H4) NN=NN+1
      DO 1 K5=1,NN
      VOL=2.*ANS(K5)+VOL
 1    CONTINUE
      K5=NN
      IF (GP(2,K1).EQ.1H4) 2,3
 2    AK=GRID*(K1-10)
      SPACE=DD5-AK
      VOL=VOL-ANS(K5)
      EXVOL=GRIDDEM*SPACE/4.*ANS(K5)
 3    DO 6 J=2,JMAX
      DO 6 K=11,K1
      IF (GP(J,K).EQ.1H2.OR.GP(J,K).EQ.1H ) GO TO 6
      K5=K5+1
      IF (GP(J,K).EQ.1H4) 4,5
 4    VD=GRIDDEM
      HD=GRID
      KF=K
      IF (GP(J+1,K).EQ.1H ) CALL VDIFF (VD)
      IF (GP(J,K-1).EQ.1H ) CALL HDIFF (Z,HD)
      IF (GP(J,K+1).EQ.1H ) CALL HDIFF (Z,HD)
      CALL FOUR (RJJ)
      IF (RJJ.EQ.1.) RJJ=3.
      VOL=VOL+RJJ*ANS(K5)
      IF (RJJ.EQ.3.) RJJ=2./3.
      EX=VD*HD/4.*RJJ*ANS(K5)
      EXVOL=EXVOL+EX
      GO TO 6
 5    IF (GP(J+1,K).EQ.1H2) EXVOL=EXVOL+ANS(K5)*GRID*GRIDDEM/8.
      IF (GP(J,K+1).EQ.1H2) EXVOL=EXVOL+ANS(K5)*GRID*GRIDDEM/8.
      IF (GP(J,K-1).EQ.1H2) EXVOL=EXVOL+ANS(K5)*GRID*GRIDDEM/8.
      VOL=VOL+4*ANS(K5)
 6    CONTINUE
      TVOL=VOL*GRID*GRIDDEM/4.+EXVOL
      TVOL=4.*TVOL
      WRITE (2,7) TVOL
      RETURN
C
 7    FORMAT (10X,*TORSIONAL CONSTANT FOR THIS BEAM*,///E12.5///)
      END
      SUBROUTINE FOUR (RJJ)
      INTEGER GP(30,90)
      COMMON /CE1/ GP,J,K,DIM,GRIDDEM,L,AK,JMAX,GRID,SQ,SQEM
      RJJ=3.
      IF (GP(J,K+1).EQ.1H ) RJJ=RJJ-1
      IF (GP(J,K-1).EQ.1H ) RJJ=RJJ-1
      IF (GP(J+1,K).EQ.1H ) RJJ=RJJ-1
```

```
      IF (GP(J-1,K).EQ.1H ) RJJ=RJJ-1
      RETURN
      END
      SUBROUTINE PTGR
C       THIS SUBROUTINE SETS INSIDE POINTS EQUAL TO 1
C       AND BOUNDARY POINTS EQUAL TO 2
      INTEGER GP(30,90)
      COMMON /CE1/ GP,J,K,DIM,GRIDDEM,L,AK,JMAX,GRID,SQ,SQEM
      K1=K+10
      IF (J.GT.JMAX) JMAX=J
      IF (J.LT.2) GO TO 3
      DO 1 J1=2,J
      GP(J1,K1)=1H1
      L=L+1
1     CONTINUE
      IF (J-1.EQ.DIM) 2,3
2     GP(J,K1)=1H2
      L=L-1
3     K=K+1
      AK=K*GRID
      RETURN
      END
      SUBROUTINE TYPE1
C       THIS SUBROUTINE WRITES THE EQUATIONS FOR THE GRID POINTS
C       WITH A VALUE OF 1
      INTEGER GP(30,90)
      COMMON /CE1/ GP,J,K,DIM,GRIDDEM,L,AK,JMAX,GRID,SQ,SQEM
      COMMON /CE2/ ANS(170),AR(170,170),KF,K1,N,K2(2)
      IF (GP(J,KF-1).EQ.1H1.OR.GP(J,KF-1).EQ.1H4) AR(N,N-1)=1./SQ
      IF (GP(J,KF+1).EQ.1H1.OR.GP(J,KF+1).EQ.1H4) AR(N,N+1)=1./SQ
      IF (GP(J+1,KF).EQ.1H1.OR.GP(J+1,KF).EQ.1H4) AR(N,N+K2(1))=1./SQEM
      AR(N,N-K2(2))=1./SQEM
      AR(N,N)=-2./SQ-2./SQEM
      ANS(N)=-2
      RETURN
      END
      SUBROUTINE TYPE3
C       THIS SUBROUTINE WRITES THE EQUATIONS FOR THE GRID POINTS
C       WITH A VALUE OF 3
      INTEGER GP(30,90)
      COMMON /CE1/ GP,J,K,DIM,GRIDDEM,L,AK,JMAX,GRID,SQ,SQEM
      COMMON /CE2/ ANS(170),AR(170,170),KF,K1,N,K2(2)
      IF (KF.EQ.K1) 1,4
1     IF (GP(J+1,K1).EQ.1H2) 2,3
2     N=N-1
      RETURN
3     CALL TYPE4
      AR(N,N+K2(1))=2.*AR(N,N+K2(1))
      RETURN
4     IF (GP(J,KF-1).EQ.1H3) AR(N,N-1)=1./SQ
      IF (GP(J,KF+1).EQ.1H3) AR(N,N+1)=1./SQ
      IF (GP(J+1,KF).EQ.1H1.OR.GP(J+1,KF).EQ.1H4) AR(N,N+K2(1))=2./SQEM
      AR(N,N)=-2./SQ-2./SQEM
      ANS(N)=-2.
      RETURN
      END
      SUBROUTINE TYPE4
C       THIS SUBROUTINE WRITES THE EQUATIONS FOR THE GRID POINTS
C       WITH A VALUE OF 4
      INTEGER GP(30,90)
      COMMON /CE1/ GP,J,K,DIM,GRIDDEM,L,AK,JMAX,GRID,SQ,SQEM
      COMMON /CE2/ ANS(170),AR(170,170),KF,K1,N,K2(2)
      COMMON /CE3/ D2,DD2,D4,D3,B,DD3,DD4,D6,D7,B8,D9,D1,DD5
      Z=0.
      VD=GRIDDEM
      HD=GRID
```

```
C       CALCULATE THE DISTANCE TO THE BORDER
      IF (GP(J+1,KF).EQ.1H ) CALL VDIFF (VD)
      IF (GP(J,KF-1).EQ.1H ) CALL HDIFF (Z,HD)
      IF (GP(J,KF+1).EQ.1H ) CALL HDIFF (Z,HD)
      ALPH1=VD/GRIDDEM
      ALPH4=HD/GRID
      IF (VD.EQ.GRIDDEM.AND.GP(J+1,KF).NE.1H2) AR(N,N+K2(1))=1./SQEM
      IF (HD.EQ.GRID.AND.GP(J,KF+1).NE.1H2) AR(N,N+1)=1./SQ
      IF (GP(J,KF).EQ.1H3) GO TO 1
      AR(N,N-K2(2))=2./((ALPH1+1)*SQEM)
    1 IF (GP(J,KF-1).NE.1H2) AR(N,N-1)=2./((ALPH4+1.)*SQ)
      AR(N,N)=-2./(ALPH1*SQEM)-2./(ALPH4*SQ)
      ANS(N)=-2.
      IF (Z.EQ.2.) 2,3
C       SWITCH THE COEFICIENTS IF THE POINT LIES IN D7
    2 Q=AR(N,N+1)
      AR(N,N+1)=AR(N,N-1)
      AR(N,N-1)=0
    3 RETURN
      END
      SUBROUTINE HDIFF (Z,HD)
C       THIS SUBROUTINE CALCULATES THE HORIZONTAL DISTANCE
C       FROM A TYPE 4 POINT TO THE BORDER
      INTEGER GP(30,90)
      COMMON /CE1/ GP,J,K,DIM,GRIDDEM,L,AK,JMAX,GRID,SQ,SQEM
      COMMON /CE2/ ANS(170),AR(170,170),KF,K1,N,K2(2)
      COMMON /CE3/ D2,DD2,D4,D3,B,DD3,DD4,D6,D7,BB,D9,D1,DD5
      AK=(KF-10)*GRID
      IF (AK.LT.DD2) 1,2
    1 X=-((J-1)*GRIDDEM-B)*D3/D4
      HD=X-AK
      Z=1.
      RETURN
    2 IF (KF.NE.K1) 3,4
    3 X=((J-1)*GRIDDEM-BB)*D7/D6
      HD=AK-X
      Z=2.
      RETURN
    4 HD=DD5-AK
      Z=3.
      RETURN
      END
      SUBROUTINE VDIFF (VD)
C       THIS SUBROUTINE CALCULATES THE VERTICLE DISTANCE
C       FROM A TYPE 4 POINT TO THE BORDER
      INTEGER GP(30,90)
      COMMON /CE1/ GP,J,K,DIM,GRIDDEM,L,AK,JMAX,GRID,SQ,SQEM
      COMMON /CE2/ ANS(170),AR(170,170),KF,K1,N,K2(2)
      COMMON /CE3/ D2,DD2,D4,D3,B,DD3,DD4,D6,D7,BB,D9,D1,DD5
      QW=(J-1)*GRIDDEM
      AK=(KF-10)*GRID
      IF (AK.LE.D2) 1,2
    1 VD=D1-QW
      RETURN
    2 IF (AK.LE.DD2) 3,4
    3 Y=-D4/D3*AK+B
      VD=Y-QW
      RETURN
    4 IF (AK.LE.DD3) 5,6
    5 VD=D1-D4-QW
      RETURN
    6 IF (AK.LE.DD4) 7,8
    7 Y=D6/D7*AK+BB
      VD=Y-QW
      RETURN
    8 VD=D9-QW
```

```
      RETURN
      END
      SUBROUTINE GETK2
C       THIS SUBROUTINE COUNTS FORWARD AND BACKWARD TO
C       FIND THE NUMBER OF EQUATIONS WRITTEN
      INTEGER GP(30,90)
      COMMON /CE1/ GP,J,K,DIM,GRIDDEM,L,AK,JMAX,GRID,SQ,SQEM
      COMMON /CE2/ ANS(170),AR(170,170),KF,K1,N,K2(2)
      NX=1
      JLL=J
1     KLL=KF
      K2(NX)=0
      K11=K1-1
      IF (GP(2,K1).EQ.1H2) K11=K1-1
      DO 4 LL=10,K11
      KLL=KLL+1
      IF (KLL.GT.K1) 2,3
2     KLL=11
      JLL=JLL+1
3     IF ((GP(JLL,KLL).EQ.1H ).OR.(GP(JLL,KLL).EQ.1H2)) GO TO 4
      K2(NX)=K2(NX)+1
4     CONTINUE
      IF (GP(J,KF).EQ.1H3) GO TO 5
      IF (NX.EQ.2) GO TO 5
      JLL=JLL-2
      NX=2
      GO TO 1
5     RETURN
      END
      SUBROUTINE SOLV1 (AR,B,N,L,DET)
C
C     ROUTINE TO SOLVE THE SYSTEM OF LINEAR
C     SIMULTANEOUS EQUATIONS A*X=B.
C
      REAL AR(170,170),B(170,1)
C
      IF (N.NE.1) GO TO 2
      DET=AR(1,1)
      DO 1 J=1,L
1     B(1,J)=B(1,J)/DET
      RETURN
2     NM1=N-1
      DET=1.0
      DO 8 I=1,NM1
      IP1=I+1
C
C     SEARCH COLUMN I FOR THE LARGEST ABSOLUTE-VALUED
C     ELEMENT IN ROWS I THROUGH N.
C
      BIG=0.0
      DO 3 J=I,N
      ABSA=ABS(AR(J,I))
      IF (BIG.GE.ABSA) GO TO 3
      BIG=ABSA
C
C     THE LARGEST ABSOLUTE-VALUED ELEMENT IS IN ROW K OF COLUMN I.
C
      K=J
3     CONTINUE
C
C     EXCHANGE ROWS K AND I, ONLY IF K IS DIFFERENT FROM I.
C
      IF (K.EQ.I) GO TO 6
      DO 4 J=I,N
      Z=AR(I,J)
      AR(I,J)=AR(K,J)
```

```
4       AR(K,J)=Z
        DO 5 J=1,L
        Z=B(I,J)
        B(I,J)=B(K,J)
5       B(K,J)=Z
C
C       CHANGE THE SIGN OF THE DETERMINANT,
C       SINCE ROWS HAVE BEEN EXCHANGED.
C
        DET=-DET
6       Z=AR(I,I)
C
C       CONTINUOUS PART-PRODUCT FOR THE DETERMINANT.
C
        DET=DET*Z
        Z=1.0/Z
C
C       MODIFY ELEMENTS OF A - THE REDUCTION PROCESS.
C       MODIFY MATRIX B ALSO.
C
        DO 8 K=IP1,N
        D=-AR(K,I)*Z
        DO 7 J=1,L
7       B(K,J)=B(K,J)+D*B(I,J)
        DO 8 J=IP1,N
8       AR(K,J)=AR(K,J)+D*AR(I,J)
        Z=AR(N,N)
C
C       FINAL VALUE OF THE DETERMINANT.
C
        DET=DET*Z
        Z=1.0/Z
C
C       PROCESS OF BACK-SUBSTITUTION TO GET THE SOLUTION MATRIX.
C
        DO 10 K=1,L
        B(N,K)=B(N,K)*Z
        DO 10 IJK=1,NM1
        I=N-IJK
        IP1=I+1
        D=0.0
        DO 9 J=IP1,N
9       D=D+AR(I,J)*B(J,K)
10      B(I,K)=(B(I,K)-D)/AR(I,I)
        RETURN
        END
```

9. ACKNOWLEDGMENTS

This study was conducted in the Department of Civil Engineering at the Fritz Engineering Laboratory, Lehigh University, Bethlehem, Pennsylvania.

The authors wish to extend their thanks to the staff of the Lehigh University Computing Center for their cooperation. Thanks is also extended to Mrs. Ruth Grimes who typed the manuscript and to Mrs. Harriet S. Kulicki for her help in proofreading it.